UNIVERSITY of York

This is a repository copy of *Magnetic Shielding Studies of C2 and C2H2 Support Higher than Triple Bond Multiplicity in C2*.

White Rose Research Online URL for this paper:
https://eprints.whiterose.ac.uk/119180/

Version: Accepted Version

Article:
Karadakov, Peter Borislavov orcid.org/0000-0002-2673-6804 and Kirsopp, Josh John Mellor (2017) Magnetic Shielding Studies of C2 and C2H2 Support Higher than Triple Bond Multiplicity in C2. Chemistry : A European Journal. pp. 12949-12954. ISSN 1521-3765

https://doi.org/10.1002/chem.201703051

Reuse
Items deposited in White Rose Research Online are protected by copyright, with all rights reserved unless indicated otherwise. They may be downloaded and/or printed for private study, or other acts as permitted by national copyright laws. The publisher or other rights holders may allow further reproduction and re-use of the full text version. This is indicated by the licence information on the White Rose Research Online record for the item.

Takedown
If you consider content in White Rose Research Online to be in breach of UK law, please notify us by emailing eprints@whiterose.ac.uk including the URL of the record and the reason for the withdrawal request.

White Rose university consortium
Universities of Leeds, Sheffield & York

eprints@whiterose.ac.uk
https://eprints.whiterose.ac.uk/

Magnetic Shielding Studies of C_2 and C_2H_2 Support Higher than Triple Bond Multiplicity in C_2

Peter B. Karadakov*[a] and Josh Kirsopp[a]

Abstract: The carbon-carbon bonds in the ground states of C_2 and C_2H_2, at their equilibrium geometries, are compared by analysing the changes in the off-nucleus magnetic shielding tensor within the space surrounding each of these molecules. A wide range of quantum-chemical approaches, including full-valence CASSCF-GIAO, CCSD(T)-GIAO and CCSDT-GIAO, all with the cc-pVQZ basis set, as well as HF-GIAO and MP2-GIAO, with the cc-pVQZ, cc-pV5Z and cc-pV6Z basis sets, show that the surroundings of the carbon-carbon bond in C_2 are more shielded than those of the carbon-carbon bond in C_2H_2. The additional shielding of the carbon-carbon bond in C_2 is found to be due to a larger paramagnetic contribution to component of the shielding tensor which is perpendicular to the molecular axis. The analysis of the off-nucleus shielding data indicates that the carbon-carbon bond in C_2 is "bulkier" and, therefore, of a higher multiplicity, but weaker than the corresponding bond in C_2H_2. According to the results of the shielding calculations, the carbon nuclei in C_2 should be much more shielded than those in C_2H_2, with ^{13}C isotropic magnetic shieldings in the *ca.* 224–227 ppm and *ca.* 123–125 ppm ranges for C_2 and C_2H_2, respectively.

Introduction

The question whether or not dicarbon, C_2, involves a quadruple carbon-carbon bond has become a major point of contention in quantum chemistry.[1–11] According to Shaik *et al.*,[1–4] in its $X^1\Sigma_g^+$ ground state C_2 features a quadruple bond comprised of two π bonds and two σ bonds. However, despite its higher multiplicity, this quadruple bond is weaker than the triple carbon-carbon bond in ground-state ethyne, C_2H_2, which has a higher force constant and a shorter bond length. A succinct account of the continuing debate surrounding the quadruple bond model of C_2 can be found in a recent review by Shaik.[12]

In this paper we compare the carbon-carbon bonds in the ground states of C_2 and C_2H_2 by analysing the changes in the off-nucleus magnetic shielding tensor, $\boldsymbol{\sigma}(\mathbf{r})$, within the space surrounding each of

[a] *Dr. P. B. Karadakov, J. Kirsopp*
Department of Chemistry, University of York
Heslington, York YO10 5DD (UK)
E-mail: peter.karadakov@york.ac.uk

these molecules. As previously observed,[13] the off-nucleus isotropic magnetic shielding, $\sigma_{\rm iso}(\mathbf{r}) = \frac{1}{3}[\sigma_{xx}(\mathbf{r}) + \sigma_{yy}(\mathbf{r}) + \sigma_{zz}(\mathbf{r})]$, exposes the differences between carbon-carbon bonds of different multiplicities in much greater detail than the total electronic density. We show that for linear molecules such as C_2 and C_2H_2 further insights are provided by the behaviour of the magnetic shielding tensor components $\sigma_\perp(\mathbf{r}) = \sigma_{xx}(\mathbf{r}) = \sigma_{yy}(\mathbf{r})$ and $\sigma_\parallel(\mathbf{r}) = \sigma_{zz}(\mathbf{r})$ which are perpendicular and parallel to the molecular axis, respectively, and the diamagnetic and paramagnetic contributions to these magnetic shielding tensor components. Additionally, we report and discuss a wide range of theoretical estimates for the carbon and proton shieldings in C_2 and C_2H_2.

Computational Procedure

All calculations on C_2 and C_2H_2 were carried out in the gas phase, at the $D_{\infty h}$ geometries from reference [14], featuring a C–C bond length of 1.2425 Å for C_2, and C–C and C–H bond lengths of 1.203 Å and 1.060 Å, respectively, for C_2H_2. Contour plots showing the variations of the off-nucleus isotropic magnetic shielding in the electronic ground states of C_2 and C_2H_2 were generated by evaluating $\boldsymbol{\sigma}(\mathbf{r})$ at regular 5 Å by 4 Å rectangular grids of points, centred on the midpoints of the respective C–C bonds, with longer sides parallel to the respective molecular axes and a spacing of 0.05 Å. The off-nucleus shielding tensors required for the contour plots were calculated using full-valence ground-state complete-active-space self-consistent field (CASSCF) wavefunctions constructed from gauge-including atomic orbitals (GIAOs), with '8 electrons in 8 orbitals' for C_2, and '10 electrons in 10 orbitals' for C_2H_2, in the standard cc-pVQZ basis set. All CASSCF-GIAO calculations were carried out using the MCSCF-GIAO (multiconfigurational SCF with GIAOs) methodology described in references [15, 16] and implemented in the Dalton program package.[17] For comparison purposes, similar contour plots for the total electron density, $\rho(\mathbf{r})$, in C_2 and C_2H_2, were drawn from the respective CASSCF(8,8)/cc-pVQZ and CASSCF(10,10)/cc-pVQZ data obtained using GAUSSIAN09.[18]

In order to study the method and basis set dependence of the off-nucleus shielding tensors in C_2 and C_2H_2, the changes in $\boldsymbol{\sigma}(\mathbf{r})$ along the respective molecular axes were examined using several additional levels of theory: MP2-GIAO (second order Møller-Plesset perturbation theory with GIAOs), in combination with the standard cc-pVQZ, cc-pV5Z and cc-pV6Z basis sets, as well as CCSD(T)-GIAO (coupled-cluster with GIAOs including all single and double excitations, and a perturbative estimate of the connected triples) and CCSDT-GIAO (CC with GIAOs including all single, double and triple excitations), both with the standard cc-pVQZ basis. All MP2-GIAO calculations were performed by means of GAUSSIAN09;[18] each of these calculations also furnished corresponding HF-GIAO (Hartree-Fock with GIAOs) results. All CCSD(T)-GIAO and CCSDT-GIAO calculations were carried out using CFOUR.[19]

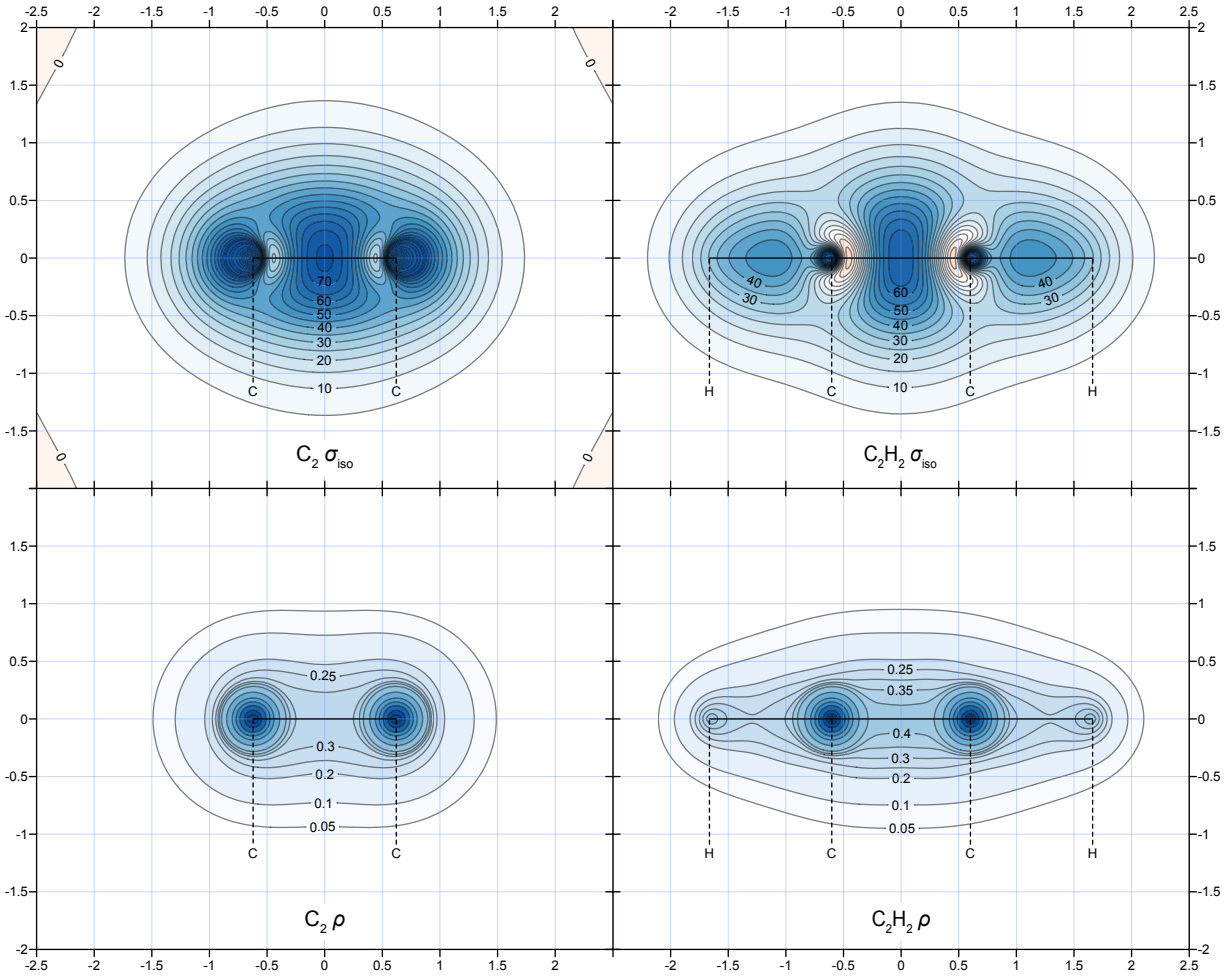

Figure 1. Isotropic shielding and total electron density contour plots in planes passing through the molecular axes of C_2 and C_2H_2. Full-valence CASSCF(8,8) (C_2) and CASSCF(10,10) (C_2H_2), cc-pVQZ basis (GIAOs for the shielding calculations), contour levels at $-10(5)80$, 90, 100, 120, 140, 160, 180, 200, 220 ppm for $\sigma_{\mathrm{iso}}(\mathbf{r})$, 0.05, 0.1, 0.2, 0.25, 0.3, 0.35. 0.4, 0.5, 1, 2.5, 5, 10, 25, 50, 75 e Bohr^{-3} for $\rho(\mathbf{r})$, axes in Å.

Results and Discussion

The isotropic magnetic shielding and total electron density contour plots for C_2 and C_2H_2 are shown in Figure 1. Looking at the total electron densities for the two molecules, it is obvious that dicarbon has less total electron density than ethyne in the region between the two carbon atoms which, of course, is an indication that C_2 has a weaker C–C bond. Somewhat surprisingly, the isotropic magnetic shielding distributions reveal a different picture: Clearly, the surroundings of the C–C bond in C_2 are more shielded than those of the C–C bond in C_2H_2. In order to link this observation to bond multiplicity, we can use the findings of a comparative study of bonding in ethane, ethene, ethyne and *s-trans*-1,3-butadiene, based on the analysis of the variations in $\sigma_{\mathrm{iso}}(\mathbf{r})$ around these molecules, which established that higher

C–C bond multiplicity is accompanied by increased shielding within the bonding region.[13] As a consequence, the higher shielding of the C–C bond in C_2 suggests that the multiplicity of this bond is higher than triple. The valence bond (VB) arguments in favour of a quadruple C–C bond in dicarbon assume that the molecule is formed from two sp hybridized carbon atoms, and involves an "inner" triple C–C bond similar to that in ethyne, as well as an "outer" forth σ bond between the second pair of "exo" sp hybrids which, in ethyne, are engaged in the two C–H bonds. The isotropic magnetic shielding distribution around C_2 (see Figure 1) shows significant shielding increases in two regions just outside the C–C bond, which are very much in the places where VB theory would put the "exo" sp hybrids. These regions are more compact than the shielded regions surrounding the C–H bonds in C_2H_2 and closer to the carbon atoms. In fact, our CASSCF(8,8)-GIAO/cc-pVQZ calculations indicate that the most shielded locations in C_2 are not at the carbon nuclei, but at points along the molecular axis at *ca*. 0.03 Å outside the C–C bond, at which $\sigma_{\rm iso}(\mathbf{r})$ reaches 232.7 ppm. From a VB viewpoint, these observations can be interpreted as an indication that the "exo" sp hybrids in C_2 remain mostly on the exterior of the C–C bonding region and have a smaller contribution to the overall C–C bond.

According to the contour plots shown in Figure 1, the most significant changes in $\sigma_{\rm iso}(\mathbf{r})$ and $\rho(\mathbf{r})$ for C_2 and C_2H_2 occur along the respective molecular axes. More detailed information about the ways in which $\sigma_{\rm iso}(\mathbf{r})$ and $\rho(\mathbf{r})$ behave as functions of distance along these axes is presented in Figures 2, 3 and 4.

Looking at the $\sigma_{\rm iso}(\mathbf{r})$ curves in Figure 2, we observe that the molecular axis of dicarbon is more shielded than that of ethyne not just along the C–C bond, but over a much wider interval between *ca.* -1 Å and 1 Å. Outside this interval, the $\sigma_{\rm iso}(\mathbf{r})$ values for ethyne become higher over the regions corresponding to the C–H bonds, and then both $\sigma_{\rm iso}(\mathbf{r})$ curves tail off to zero in a similar fashion. While it was not unexpected that the carbons in C_2 would be more shielded than those in C_2H_2, the magnitude of the difference at the full-valence CASSCF-GIAO/cc-pVQZ level, 226.62 ppm vs. 132.87 ppm, comes as a surprise. Another interesting related feature of the isotropic magnetic shielding distribution in C_2 (see Figures 1 and 2) is the absence of deshielded "halos" such as those observed previously around carbon atoms which are sp or sp^2 hybridized[13,20–23] (this effect does not occur around sp^3 hybridized carbon atoms[13]). Clearly, $\sigma_{\rm iso}(\mathbf{r})$ in C_2 shows some depressions along and around the C–C bond, close to each carbon atom, but these depressions are not deep enough to give rise to regions of negative $\sigma_{\rm iso}(\mathbf{r})$ values (or, deshielded "halos") as in C_2H_2.

The $\sigma_\perp(\mathbf{r})$ and $\sigma_\parallel(\mathbf{r})$ components of the magnetic shielding tensors for C_2 and C_2H_2 show rather different types of behaviour along the respective molecular axes (see Figure 2). The shapes of the $\sigma_\perp(\mathbf{r})$ curves resemble those for $\sigma_{\rm iso}(\mathbf{r})$, but the distinction between C_2 and C_2H_2 is more pronounced, especially along the C–C bonds where the higher C_2 curve emphasizes the greater "bulk" of shielding

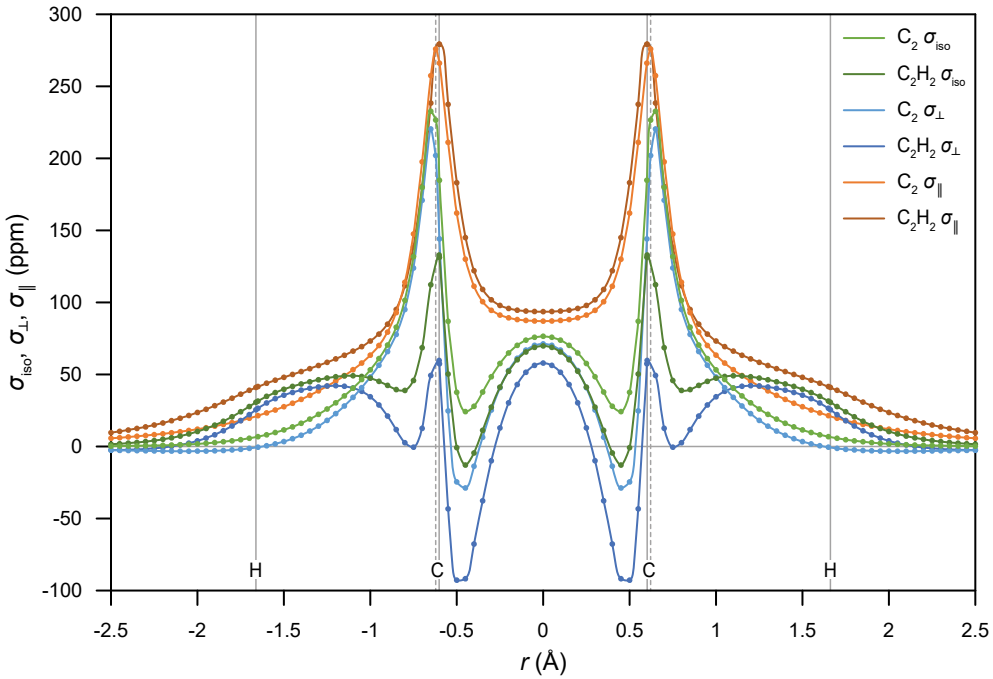

Figure 2. Isotropic shielding and components of the shielding tensor along the molecular axes of C_2 and C_2H_2 (wavefunctions as for Figure 1, vertical lines denote the positions of the carbon and hydrogen atoms, dotted lines for C_2).

around the respective bond; this is consistent with the notion of a bond of higher multiplicity than in C_2H_2. For each of C_2 and C_2H_2, $\sigma_\parallel(\mathbf{r})$ is a positive function along the corresponding molecular axis, with sharp peaks at the positions of the carbon atoms only. Except for a narrow interval next to each carbon and outside the C–C bond, $\sigma_\parallel(\mathbf{r})$ in C_2H_2 is higher than in C_2. This finding can be explained by the additional shielding along the molecular axis caused by the presence of the hydrogen atoms. Our CASSCF(10,10)-GIAO/cc-pVQZ $\sigma_{\mathrm{iso}}(\mathbf{r})$, $\sigma_\perp(\mathbf{r})$ and $\sigma_\parallel(\mathbf{r})$ curves for C_2H_2 are qualitatively very similar to those obtained by Wolinski at the HF-GIAO/6-311G** level of theory;[24] the higher level of theory used in the current work introduces only relatively minor quantitative changes.

It is also instructive to examine the plots of the components of the diamagnetic and paramagnetic contributions to the magnetic shielding tensors for C_2 and C_2H_2, $\boldsymbol{\sigma}(\mathbf{r}) = \boldsymbol{\sigma}^{\mathrm{d}}(\mathbf{r}) + \boldsymbol{\sigma}^{\mathrm{p}}(\mathbf{r})$, along the respective molecular axes, shown in Figure 3. Note that Figure 3 does not include $\sigma_\parallel^{\mathrm{p}}(\mathbf{r})$ plots as this quantity is equal to zero in linear molecules; as a consequence, in C_2 and C_2H_2 $\sigma_\parallel(\mathbf{r}) = \sigma_\parallel^{\mathrm{d}}(\mathbf{r})$ and the corresponding plots in Figures 2 and 3 are identical. As emphasized by Wolinski,[24] the partitioning of the magnetic shielding tensor into diamagnetic and paramagnetic contributions is not a unique procedure; our CASSCF-GIAO results utilize the "natural connection"[25,26] implemented as default in Dalton[17] and cannot be compared to those from reference [24] which were obtained using a different partitioning. In general, the diamagnetic contribution to the magnetic shielding tensor depends on

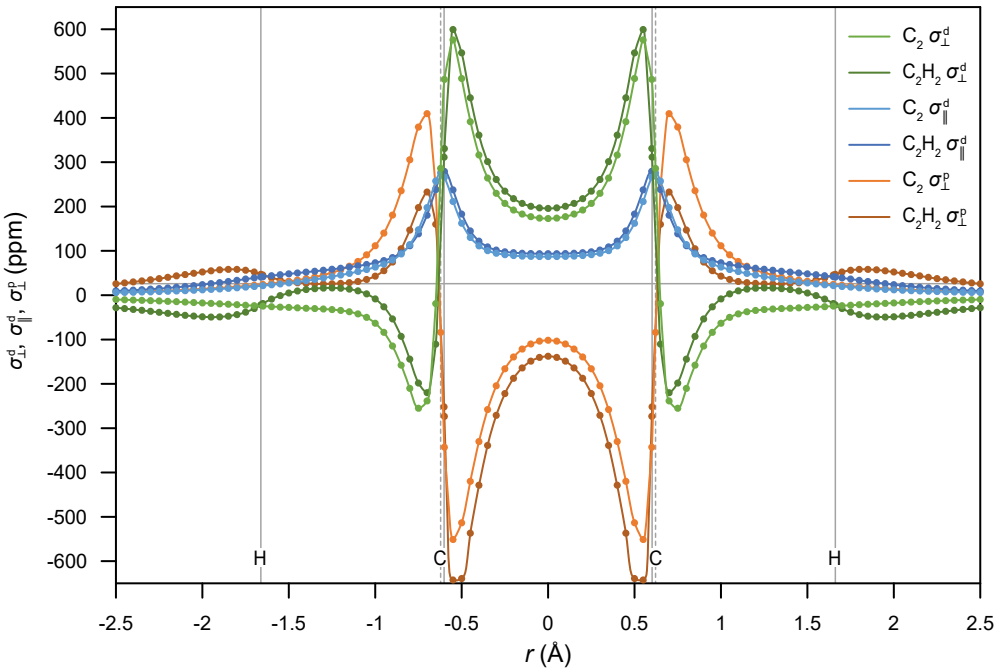

Figure 3. Diamagnetic and paramagnetic contributions to the components of the shielding tensor along the molecular axes of C_2 and C_2H_2 (wavefunctions as for Figure 1, other details as in Figure 2).

the total electron density of the unperturbed wavefunction only, whereas the paramagnetic contribution involves the first-order correction to the wavefunction in response to the perturbation caused by the external magnetic field (for a more detailed analysis, see *e.g.* reference [25]). As the total electron density of the full-valence CASSCF/cc-pVQZ wavefunction for C_2H_2 along the molecular axis is higher than that of the corresponding wavefunction for C_2, except for a narrow interval next to each carbon and outside the C–C bond (see Figure 4), we can expect similar behaviour of the $\sigma_\perp^{\mathrm{d}}(\mathbf{r})$ and $\sigma_\parallel^{\mathrm{d}}(\mathbf{r})$ curves for the two molecules; Figure 3 confirms that this is, indeed, the case. Thus, the extra shielding of the C–C bond in C_2 can be attributed to the $\sigma_\perp^{\mathrm{p}}(\mathbf{r})$ contribution to the magnetic shielding tensor. This is an indication that the wavefunction for C_2 is easier to perturb by an external magnetic field than that for C_2H_2, in a direction perpendicular to the C–C bond, which is in line with the idea of a weaker but "bulkier" C–C bond in C_2.

The shapes of the total electron density plots for C_2 and C_2H_2 along the respective molecular axes (see Figure 4) are very much as expected, with high peaks over the positions of the carbon atoms and much lower peaks over the positions of the hydrogen atoms in ethyne. Interestingly, the $\rho(\mathbf{r})$ values at the positions of the carbon atoms in C_2 are slightly higher than the corresponding values in C_2H_2, 124.21 against 123.77 e Bohr^{-3}, respectively, and, as noted earlier, $\rho(\mathbf{r})$ for C_2 remains higher than that for C_2H_2 over short intervals outside the C–C bond region.

The more general features of the magnetic shielding distributions in C_2 and C_2H_2, calculated at the

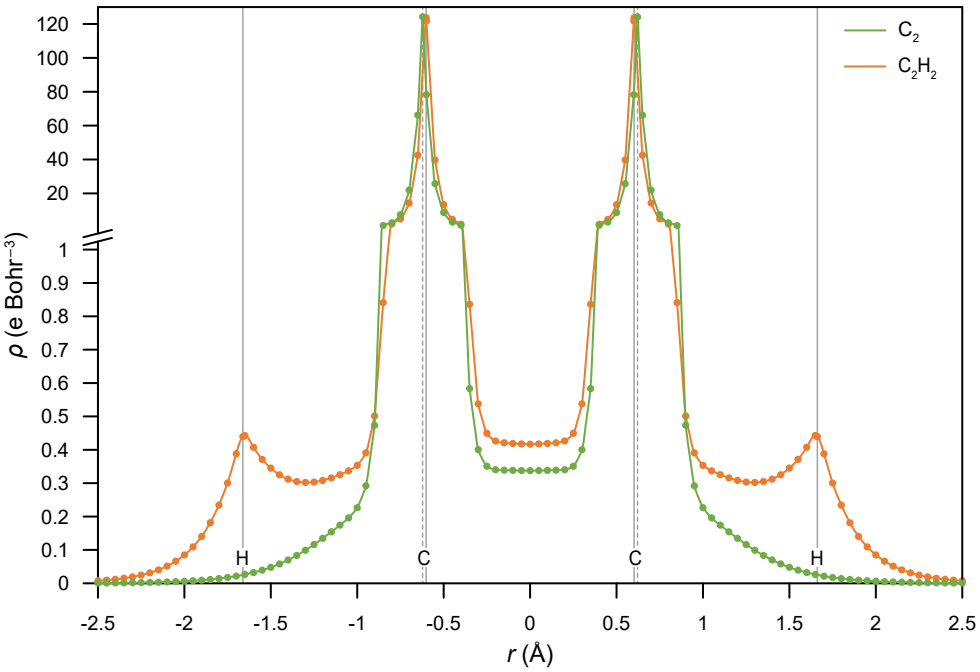

Figure 4. Total electron density along the molecular axes of C_2 and C_2H_2 (wavefunctions as for Figure 1, other details as in Figure 2). The $\rho(\mathbf{0})$ values (at the midpoints of the C–C bonds) are 0.42 and 0.34 e Bohr^{-3}, respectively.

respective full-valence CASSCF-GIAO/cc-pVQZ levels of theory, are also reproduced at other levels of theory. In Figure 5, we compare the full-valence CASSCF-GIAO/cc-pVQZ curves for the isotropic magnetic shielding along the molecular axes of C_2 and C_2H_2 to the corresponding curves obtained at the HF-GIAO, MP2-GIAO, CCSD(T)-GIAO and CCSDT-GIAO levels of theory, within the same basis set. The more pronounced differences between the $\sigma_{\mathrm{iso}}(\mathbf{r})$ curves shown in Figure 5 are at and around the carbon nuclei, and at and around the $\sigma_{\mathrm{iso}}(\mathbf{r})$ local minima near either end of each C–C bonding region. Once outside the interval between *ca.* -1 Å and 1 Å, the differences between the $\sigma_{\mathrm{iso}}(\mathbf{r})$ curves become very small (this is also true of the regions surrounding the positions of the hydrogens in C_2H_2). The differences between the $\sigma_{\mathrm{iso}}(\mathbf{r})$ curves become smaller also around the midpoints of the C–C bonds but the HF-GIAO curves for both C_2 and C_2H_2, and the MP2-GIAO curve for C_2 can be seen to pass noticeably higher than the remaining three curves. This is an indication that inclusion of certain types of correlation effects can be required for obtaining accurate magnetic shielding results not only at nuclear positions, but also along multiple bonds. The HF-GIAO and MP2-GIAO $\sigma_{\mathrm{iso}}(\mathbf{r})$ curves obtained using the cc-pV5Z and cc-pV6Z basis sets are not shown in Figure 5 as these curves are almost indistinguishable from the corresponding curves in the cc-pVQZ basis set everywhere except at and very close to the positions of the carbon and hydrogen atoms.

Numerical data about the isotropic magnetic shieldings for the carbon and hydrogen nuclei and

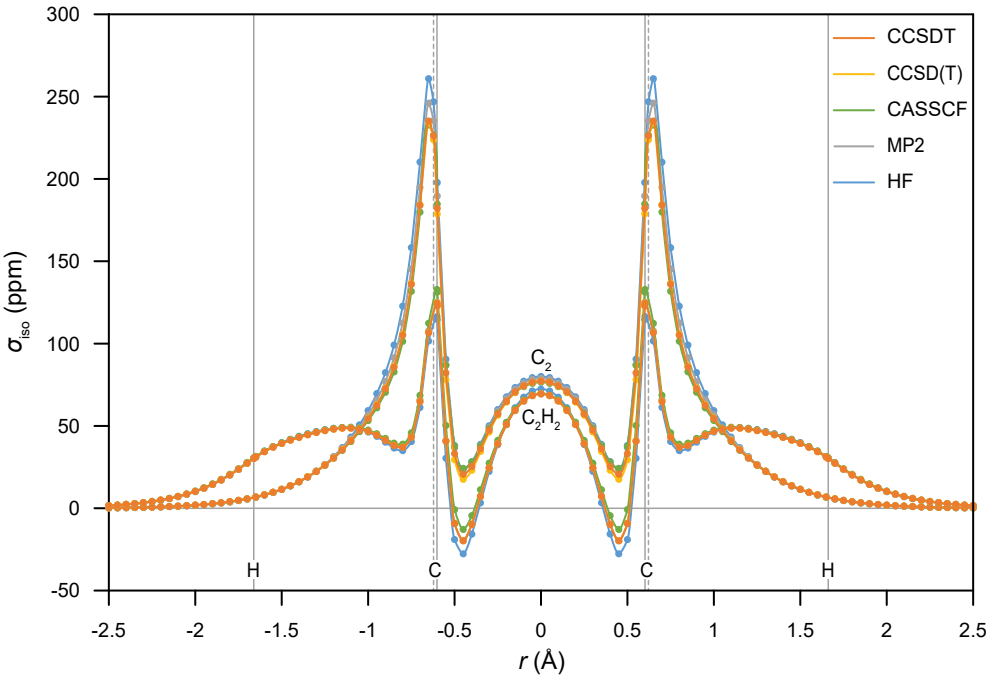

Figure 5. Isotropic shielding along the molecular axes of C_2 and C_2H_2, calculated using the CCSDT-GIAO, CCSD(T)-GIAO, CASSCF-GIAO, MP2-GIAO and HF-GIAO methods, within the cc-pVQZ basis (other details as in Figure 2).

the midpoints of the C–C bonds in dicarbon and ethyne, $\sigma_{iso}(^{13}C)$, $\sigma_{iso}(^{1}H)$ and $\sigma_{iso}(\mathbf{0})$, respectively, calculated at the various levels of theory employed in the current work, are collected in Table 1. The data highlight the differences in performance between the methods we used in the shielding calculations on the two molecules; most of these differences can be attributed to the well-known fact that, while the single-determinant closed-shell HF wavefunction works reasonably well for ethyne, it does not provide a particularly good description of the electronic structure of dicarbon.

Looking at the calculations performed within the cc-pVQZ basis set, it is clear that the HF-GIAO estimate for the isotropic magnetic shielding of a carbon nucleus in C_2 is way too high; the corresponding MP2-GIAO value shows some improvement but the adverse effect of using a closed-shell HF reference is eliminated only in the CCSD(T)-GIAO and CCSDT-GIAO results, which are reasonably close and in good agreement with their CASSCF(8,8)-GIAO counterpart. It is somewhat unexpected to observe that, in this case, the full-valence CASSCF(8,8)-GIAO and CCSDT-GIAO methods introduce very similar electron-correlation corrections to $\sigma_{iso}(^{13}C)$, adjusting the HF-GIAO value downwards by -20.23 ppm and -20.67 ppm, respectively, the CCSD(T)-GIAO result is even lower (electron-correlation correction of -23.02 ppm), whereas MP2-GIAO manages a much more modest electron-correlation correction of only -11.47 ppm. The method dependence of the theoretical estimate for the ^{13}C isotropic magnetic shielding in ethyne is more conventional: HF-GIAO and full-valence CASSCF(10,10)-GIAO underes-

Table 1. Isotropic magnetic shieldings for carbon and hydrogen nuclei and the midpoints of the C–C bonds in dicarbon and ethyne (in ppm).

Method	C_2		C_2H_2		
	$\sigma_{iso}(^{13}C)$	$\sigma_{iso}(\mathbf{0})$	$\sigma_{iso}(^{13}C)$	$\sigma_{iso}(^{1}H)$	$\sigma_{iso}(\mathbf{0})$
CASSCF-GIAO/cc-pVQZ[a]	226.62	76.49	132.87	30.66	69.77
CCSD(T)-GIAO/cc-pVQZ	223.83	77.27	124.87	30.22	69.50
CCSDT-GIAO/cc-pVQZ	226.18	77.20	124.56	30.23	69.51
HF-GIAO/cc-pVQZ	246.85	80.00	116.41	30.36	72.38
HF-GIAO/cc-pV5Z	246.56	80.07	114.93	31.21	72.42
HF-GIAO/cc-pV6Z	246.60	80.08	114.68	31.20	72.42
MP2-GIAO/cc-pVQZ	235.38	78.87	125.17	30.16	69.38
MP2-GIAO/cc-pV5Z	234.85	78.97	123.25	30.97	69.48
MP2-GIAO/cc-pV6Z	234.76	78.99	122.85	30.95	69.51

[a] CASSCF(8,8)-GIAO for C_2; CASSCF(10,10)-GIAO for C_2H_2.

timate and overestimate, respectively, this quantity, in a manner similar to that observed in HF-GIAO and CASSCF(6,6)-GIAO shielding calculations on benzene.[27] The MP2-GIAO, CCSD(T)-GIAO and CCSDT-GIAO results for $\sigma_{iso}(^{13}C)$ in ethyne are very close, spaced by just *ca.* 0.3 ppm, with MP2-GIAO yielding the largest and CCSDT-GIAO the smallest value. Our MP2-GIAO and CCSD(T)-GIAO ^{13}C isotropic magnetic shieldings for ethyne are in good agreement with the value of 123.5 pm obtained by Auer *et al.*[29] for both the MP2-GIAO and CCSD(T)-GIAO methods, using a quadruple-ζ basis set denoted as qz2p at the CCSD(T)/cc-pVTZ optimized geometry.

Method choice affects the $\sigma_{iso}(\mathbf{0})$ results for both C_2 and C_2H_2 less than those for $\sigma_{iso}(^{13}C)$: The differences between the highest and lowest $\sigma_{iso}(\mathbf{0})$ estimates amount to 3.51 ppm for C_2, between the HF-GIAO and CASSCF(8,8)-GIAO results, and to 3.00 ppm for C_2H_2, between the HF-GIAO and MP2-GIAO results, respectively. The method dependence of the proton isotropic magnetic shieldings in C_2H_2 is even weaker: The largest difference of 0.50 ppm is observed between the results obtained using the CASSCF(10,10)-GIAO and MP2-GIAO methods.

As shown by the data included in Table 1, when using the HF-GIAO and MP2-GIAO methods, increasing the basis set size in the sequence cc-pVQZ, cc-pV5Z, cc-pV6Z makes the midpoints of the C–C bonds in both dicarbon and ethyne more shielded, but the changes are very small: The largest overall change of 0.13 ppm is observed in the MP2-GIAO $\sigma_{iso}(\mathbf{0})$ values for ethyne. The basis set dependence of the HF-GIAO and MP2-GIAO results for $\sigma_{iso}(^{13}C)$ in C_2 and $\sigma_{iso}(^{1}H)$ in C_2H_2 is also

relatively weak, but not entirely as expected: The MP2-GIAO $\sigma_{iso}(^{13}C)$ value in C_2 decreases all the way on increasing the size of the basis set, by 0.62 ppm overall, but the HF-GIAO $\sigma_{iso}(^{13}C)$ value in C_2 and the HF-GIAO and MP2-GIAO $\sigma_{iso}(^{1}H)$ values in C_2H_2 show small decreases on passing from the cc-pVQZ to the cc-pV5Z basis set, but these are then followed by increases of much smaller magnitudes on continuing to the cc-pV6Z basis set. The most pronounced basis set dependence amongst the quantities included in Table 1 is exhibited by the ^{13}C isotropic magnetic shielding in ethyne: The corresponding HF-GIAO and MP2-GIAO estimates decrease, by 1.48 ppm and 1.92 ppm, respectively, on switching from the cc-pVQZ to the cc-pV5Z basis set, and by further 0.25 ppm and 0.40 ppm, respectively, on switching from the cc-pV5Z to the cc-pV6Z basis set.

A theoretical estimate of the ^{13}C isotropic magnetic shielding in ethyne which agrees very well with the experimental absolute gas-phase shielding of 117.2 ppm (at 300 K, extrapolated to zero pressure)[28] can be obtained from the results reported by Auer *et al.*,[29] by combining the CCSD(T)-GIAO/13s9p4d3f// CCSD(T)/cc-pVTZ shielding of 122.6 ppm with the zero-point vibrational correction of -3.84 ppm, evaluated at the CCSD(T)-GIAO/qz2p//CCSD(T)/cc-pVTZ level, which yields 118.8 ppm. According to the results of the current work, in the cc-pVQZ basis set the CCSDT-GIAO estimate for $\sigma_{iso}(^{13}C)$ in ethyne is 0.31 ppm lower than its CCSD(T)-GIAO counterpart. While this is a change in the right direction, at this stage it is not possible to predict whether the use of CCSDT-GIAO rather than CCSD(T)-GIAO throughout, within a very large basis set, plus a thermal correction,[30] would be sufficient to eliminate the remaining difference between the experimental and theoretical values.

Conclusions

Off-nucleus shielding calculations on dicarbon and ethyne carried out using a wide range of quantum-chemical approaches, including full-valence CASSCF-GIAO, CCSD(T)-GIAO and CCSDT-GIAO, all with the cc-pVQZ basis set, as well as HF-GIAO and MP2-GIAO, with the cc-pVQZ, cc-pV5Z and cc-pV6Z basis sets, show that the surroundings of the carbon-carbon bond in dicarbon are more shielded than those of the carbon-carbon bond in ethyne. The off-nucleus isotropic magnetic shielding, $\sigma_{iso}(\mathbf{r})$, for each of these molecules reaches a local maximum at the midpoint of the respective carbon-carbon bond; the isotropic shielding of the midpoint of the C–C bond in C_2, $\sigma_{iso}(\mathbf{0})$, is between *ca.* 9.6% and 13.7% higher (at the full-valence CASSCF-GIAO/cc-pVQZ and MP2-GIAO/ccpVQZ levels of theory, respectively, see Table 1) than its counterpart in C_2H_2. The behaviour of the total electron density, $\rho(\mathbf{r})$, evaluated at the full-valence CASSCF-GIAO/cc-pVQZ level of theory, in both dicarbon and ethyne is rather dissimilar: Dicarbon has less total electron density than ethyne along and around the carbon-carbon bond, and the midpoint of the carbon-carbon bond in each molecule corresponds to a

second-order saddle point of $\rho(\mathbf{r})$; away from the midpoint, $\rho(\mathbf{r})$ increases along the molecular axis and decreases in any direction perpendicular to the molecular axis. The difference between the total electron densities at the midpoints of the C–C bonds in C_2 and C_2H_2 is more pronounced than the corresponding $\sigma_{iso}(\mathbf{0})$ difference: $\rho(\mathbf{0})$ in C_2H_2 is *ca.* 23.5% higher than its C_2 counterpart (see Figure 4).

The in-depth analysis of the changes in the composition of the off-nucleus magnetic shielding tensor, $\boldsymbol{\sigma}(\mathbf{r})$, along the molecular axes of C_2 and C_2H_2, carried out at the full-valence CASSCF-GIAO/cc-pVQZ level of theory, reveals that the increased shielding of the carbon-carbon bond in C_2 is due to two interrelated factors: Firstly, the values of the shielding tensor component perpendicular to the molecular axis, $\sigma_{\perp}(\mathbf{r})$, are higher in C_2 and, secondly, this comes as the consequence of a larger paramagnetic contribution to $\sigma_{\perp}(\mathbf{r})$, $\sigma^{p}_{\perp}(\mathbf{r})$ (see Figures 2 and 3). Both of these factors suggest that C_2 incorporates a "bulkier" C–C bond; additionaly, since the larger $\sigma^{p}_{\perp}(\mathbf{r})$ in C_2 implies that its wavefunction is easier to perturb by an external magnetic field than that for C_2H_2, in a direction perpendicular to the C–C bond, the C–C bond in C_2 should be weaker.

These findings, when combined with the link between carbon-carbon bond multiplicity and extent of isotropic magnetic shielding within the bonding region established in reference [13], lend support to the idea that the weaker carbon-carbon bond in C_2 can be of higher multiplicity than the stronger carbon-carbon bond in C_2H_2.

The current work makes no predictions about the individual σ and π bonds that may contribute to the multiple carbon-carbon bonds in dicarbon and ethyne. In fact, it is debatable whether the σ-π bond model should be preferred over the alternative "bent" bond model which, in spin-coupled calculations, yields a lower-energy wavefunction for ethyne.[31] On a side note, Foster-Boys localizations[32] of the active space orbitals from the full-valence CASSCF(8,8)/cc-pVQZ and CASSCF(10,10)/cc-pVQZ wavefunctions for dicarbon and ethyne, respectively, carried out using GAUSSIAN09,[18] produce rather similar sets of localized orbitals consistent with the "bent" bond model.

All quantum-chemical approaches employed in the current work predict that the carbon nuclei in dicarbon should be much more shielded that those in ethyne (see Table 1). The theoretical estimates for the carbon isotropic magnetic shieldings in dicarbon obtained using the CASSCF(8,8)-GIAO, CCSD(T)-GIAO and CCSDT-GIAO methods are in good agreement, within the *ca.* 224–227 ppm range, but the HF-GIAO and MP2-GIAO results are considerably higher (see Table 1). On the other hand, the MP2-GIAO, CCSD(T)-GIAO and CCSDT-GIAO methods yield similar $\sigma_{iso}(^{13}C)$ values fo ethyne, within the *ca.* 123–125 ppm range, very much in-between the higher CASSCF(10,10)-GIAO and lower HF-GIAO results. Two methods, CCSDT-GIAO and CCSD(T)-GIAO, are identified to be performing uniformly well in the calculation of ^{13}C shieldings for both dicarbon and ethyne.

It would be very interesting to see if the theoretical estimates for the ^{13}C isotropic magnetic shield-

ings in dicarbon reported in the current work could be verified by gas phase NMR measurements, as this would provide experimental support for the conclusions made on the basis of the respective magnetic shielding calculations. This would be an useful addition to the short list of potentially measureable experimetal properties that can be used to discuss the nature of bonding in dicarbon; another example of a property of this type is the enthalpy of the forth carbon-carbon bond in C_2 which has been estimated as 16.8 $kcal^{-1}$ from the thermochemistry of the reactions $HCCH \rightarrow HCC\cdot + \cdot H \rightarrow C_2 + \cdot H$.[2]

Conflict of interest

The authors declare no conflict of interest.

Keywords: bond multiplicity in C_2 · off-nucleus magnetic shielding tensor · ^{13}C isotropic magnetic shielding · quadruple bond · dicarbon · ethyne

[1] S. Shaik, D. Danovich, W. Wu, P. Su, H. S. Rzepa, P. C. Hiberty, *Nat. Chem.* **2012**, *4*, 195–200.

[2] S. Shaik, H. S. Rzepa, R. Hoffmann, *Angew. Chem. Int. Ed.* **2013**, *52*, 3020–3033.

[3] D. Danovich, P. C. Hiberty, W. Wu, H. S. Rzepa, S. Shaik, *Chem. Eur. J.* **2014**, *20*, 6220–6232.

[4] S. Shaik, D. Danovich, Benoit Braida, P. C. Hiberty, *Chem. Eur. J.* **2016**, *22*, 4116–4128.

[5] P. v. R. Schleyer, P. Maslak, J. Chandrasekhar, R. Grev, *Tetrahedron Lett.* **1993**, *34*, 6387–6390.

[6] G. Frenking, M. Hermann, *Chem. Eur. J.* **2016**, *22*, 18975–18976.

[7] S. Shaik, D. Danovich, B. Braida, P. C. Hiberty, *Chem. Eur. J.* **2016**, *22*, 18977âĂŞ18980.

[8] W. Zou, D. Cremer, *Chem. Eur. J.* **2016**, *22*, 4087–4099.

[9] L. T. Xu, T. H. Dunning, Jr., *J. Chem. Theory Comput.* **2014**, *10*, 195–201.

[10] D. L. Cooper, F. E. Penotti, R. Ponec, *Comput. Theoret. Chem.* **2015**, *1053*, 189–194.

[11] D. W. O. de Sousa, M. A. C. Nascimento, *J. Chem. Theory Comput.* **2016**, *12*, 2234–2241.

[12] S. Shaik, *Comput. Theoret. Chem.* **2017**, DOI: 10.1016/j.comptc.2017.02.011.

[13] P. B. Karadakov, K. E. Horner, *J. Chem. Theory Comput.* **2016**, *12*, 558–563.

[14] D. R. Lide, *Structure of Free Molecules in the Gas Phase*, in *CRC Handbook of Chemistry and Physics, 96th Edition (Internet Version 2016)*, (Ed.: W. M. Haynes), CRC Press/Taylor and Francis, Boca Raton, FL.

[15] K. Ruud, T. Helgaker, R.Kobayashi, P. Jørgensen, K. L. Bak, H. J. A. Jensen, *J. Chem. Phys.* **1994**, *100*, 8178–8185.

[16] K. Ruud, T. Helgaker, K. L. Bak, P. Jørgensen, P.; J. Olsen, *Chem. Phys.* **1995**, *195*, 157–169.

[17] K. Aidas, C. Angeli, K. L. Bak, V. Bakken, R. Bast, L. Boman, O. Christiansen, R. Cimiraglia, S. Coriani, P. Dahle, E. K. Dalskov, U. Ekström, T. Enevoldsen, J. J. Eriksen, P. Ettenhuber, B. Fernández, L. Ferrighi, H. Fliegl, L. Frediani, K. Hald, A. Halkier, C. Hättig, H. Heiberg, T. Helgaker, A. C. Hennum, H. Hettema, R. Hjertenæs, S. Høst, I.-M. Høyvik, M. F. Iozzi, B. Jansík, H. J. Aa. Jensen, D. Jonsson, P. Jørgensen, J. Kauczor, S. Kirpekar, T. Kjærgaard, W. Klopper, S. Knecht, R. Kobayashi, H. Koch, J. Kongsted, A. Krapp, K. Kristensen, A. Ligabue, O. B. Lutnæs, J. I. Melo, K. V. Mikkelsen, R. H. Myhre, C. Neiss, C. B. Nielsen, P. Norman, J. Olsen, J. M. H. Olsen, A. Osted, M. J. Packer, F. Pawlowski, T. B. Pedersen, P. F. Provasi, S. Reine, Z. Rinkevicius, T. A. Ruden, K. Ruud, V. V. Rybkin, P. Sałek, C. C. M. Samson, A. Sánchez de Merás, T. Saue, S. P. A. Sauer, B. Schimmelpfennig, K. Sneskov, A. H. Steindal, K. O. Sylvester-Hvid, P. R. Taylor, A. M. Teale, E. I. Tellgren, D. P. Tew, A. J. Thorvaldsen, L. Thøgersen, O. Vahtras, M. A. Watson, D. J. D. Wilson, M. Ziolkowski, H. Ågren, *WIREs Comput. Mol. Sci.* **2014**, *4*, 269–284; *Dalton, a Molecular Electronic Structure Program, Release Dalton2016.2 (2015)*, see http://daltonprogram.org.

[18] M. J. Frisch, G. W. Trucks, H. B. Schlegel, G. E. Scuseria, M. A. Robb, J. R. Cheeseman, G. Scalmani, V. Barone, B. Mennucci, G. A. Petersson, H. Nakatsuji, M. Caricato, X. Li, H. P. Hratchian, A. F. Izmaylov, J. Bloino, G. Zheng, J. L. Sonnenberg, M. Hada, M. Ehara, K. Toyota, R. Fukuda, J. Hasegawa, M. Ishida, T. Nakajima, Y. Honda, O. Kitao, H. Nakai, T. Vreven, J. A. Montgomery Jr., J. E. Peralta, F. Ogliaro, M. Bearpark, J. J. Heyd, E. Brothers, K. N. Kudin, V. N. Staroverov, R. Kobayashi, J. Normand, K. Raghavachari, A. Rendell, J. C. Burant, S. S. Iyengar, J. Tomasi, M. Cossi, N.Rega, J. M. Millam, M. Klene, J. E. Knox, J. B. Cross, V. Bakken, C. Adamo, J. Jaramillo, R. Gomperts, R. E. Stratmann, O. Yazyev, A. J. Austin, R. Cammi, C. Pomelli, J. W. Ochterski, R. L. Martin, K. Morokuma, V. G. Zakrzewski, G. A. Voth, P. Salvador, J. J. Dannenberg, S. Dapprich, A. D. Daniels, Ö. Farkas, J. B. Foresman, J. V. Ortiz, J. Cioslowski, D. J. Fox, *Gaussian 09, Revision D.01*, Gaussian, Inc., Wallingford, CT, **2009**.

[19] J. F. Stanton, J. Gauss, M. E. Harding, P. G. Szalay, with contributions from A. A. Auer, R. J. Bartlett, U. Benedikt, C. Berger, D. E. Bernholdt, Y. J. Bomble, L. Cheng, O. Christiansen O., M. Heckert, O. Heun, C. Huber, T.-C. Jagau, D. Jonsson, J. Jusélius, K. Klein, W. J. Lauderdale, D. A. Matthews, T. Metzroth, L. A. Mück, D. P. O'Neill, D. R. Price, E. Prochnow, C. Puzzarini, K. Ruud, F. Schiffmann, W. Schwalbach, C. Simmons, S. Stopkowicz, A. Tajti, J. Vázquez, F.

Wang, J. D. Watts, and the integral packages MOLECULE (J. Almlöf, P. R. Taylor), PROPS (P. R. Taylor), ABACUS (T. Helgaker, H. J. Aa. Jensen, P. Jørgensen, J. Olsen,), and ECP routines by A. V. Mitin, C. van Wüllen, *CFOUR, Coupled-Cluster Techniques for Computational Chemistry, a Quantum-Chemical Program Package*, see http://www.cfour.de.

[20] P. B. Karadakov, K. E. Horner, *J. Phys. Chem. A* **2013**, *117*, 518–523.

[21] K. E. Horner, P. B. Karadakov, *J. Org. Chem.* **2013**, *78*, 8037–8043.

[22] K. E. Horner, P. B. Karadakov, *J. Org. Chem.* **2015**, *80*, 7150–7157.

[23] P. B. Karadakov, P. Hearnshaw, K. E. Horner, *J. Org. Chem.* **2015**, *81*, 11346–11352.

[24] K. Wolinski, *J. Chem. Phys.* **1997**, *106*, 6061–6067.

[25] J. Olsen, K. L. Bak, K. Ruud, T. Helgaker, P. Jørgensen, *Theor. Chim. Acta* **1995**, *90*, 421–439.

[26] K. Ruud, T. Helgaker, J. Olsen, P. Jørgensen, K. L. Bak, *Chem. Phys. Lett.* **1995**, *235*, 47–52.

[27] P. B. Karadakov, *J. Phys. Chem. A* **2008**, *112*, 7303–7309.

[28] A. K. Jameson, C. J. Jameson, *Chem. Phys. Lett.* **1987**, *134*, 461–466.

[29] A. A. Auer, J. Gauss, J. F. Stanton, *J. Chem. Phys.* **2003**, *118*, 10407–10417.

[30] D. Sundholm, J. Gauss, A. Schäfer, *J. Chem. Phys.* **1996**, *105*, 11051–11059.

[31] P. B. Karadakov, J. Gerratt, D. L. Cooper, M. Raimondi, *J. Am. Chem. Soc.* **1993**, *115*, 6863–6869.

[32] J. M. Foster and S. F. Boys, *Rev. Mod. Phys.*, **1960**, *32*, 300–302.

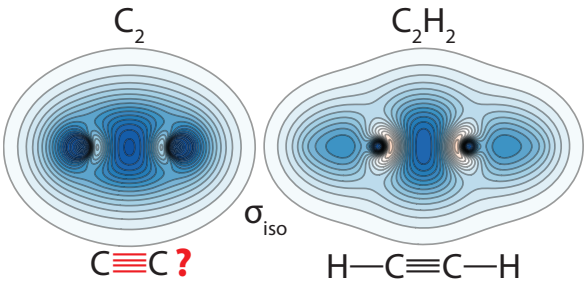

Is there a quadruple carbon-carbon bond in C_2? Off-nucleus shielding calculations indicate that the carbon-carbon bond in C_2 is more shielded than the triple carbon-carbon bond in C_2H_2 and can, therefore, have higher than triple bond multiplicity.